Chemistry Modifications of Inconel 706 for Improved Microstructural Stability

D. Del Genovese[1], D. Mukherji[1], J. Rösler[1], V. Kindrachuk[2], N. Wanderka[2] and J. Banhart[2]

[1] Institut für Werkstoffe, TU Braunschweig, Langer Kamp 8, 38106 Braunschweig, Germany
[2] Hahn-Meitner-Institut Berlin, Glienickerstr. 100, 14109 Berlin, Germany

Due to its combination of high mechanical strength with good fabricability and machinability, Inconel 706 is under consideration for ultra high temperature steam turbine applications with prospective steam temperatures up to 973 K. The alloy properties directly depend on the precipitation hardening system, which is based on the coherent precipitation of two kinds of A_3B-type compounds: the fcc $Ni_3[Ti,Nb,Al]$ γ' phase and the bct $Ni_3[Nb,Ti]$ γ'' phase. However, the γ' and γ'' precipitates in this alloy exhibit a metastable character, and transform to large laths of η phase (hcp $Ni_3[Ti,Nb]$) upon exposure at $T > 923$ K. This overageing process is accompanied by an unacceptable loss of creep and tensile strength. In order to overcome this impasse, two different stabilization concepts were probed. On the one hand, it was attempted to create a diffusion barrier in the matrix surrounding the γ'/γ'' precipitates by adding Rhenium to the composition of Inconel 706. Rhenium is known to effectively retard the γ' coarsening in cast single crystal Ni-base superalloys, as it strongly partitions to the matrix. On the other hand, the [Ti+Al]/[Nb] ratio of Inconel 706 was specifically refined in order to minimize the thermodynamical tendency to transformation of γ'/γ''. This modification was associated with a redesign of the Inconel 706 chemistry, resulting in a new alloy, named DT706.
The microstructures of Inconel 706, Re-modified 706, and DT706 were investigated by means of electron microscopy (SEM, TEM) and three-dimensional atom probe (3DAP) in the as-heat treated condition as well as after long-term exposure at 1023 K. Results show that Rhenium was homogeneously dissolved in the matrix, but its partitioning ratio is too low to provide an effective obstacle to the γ'/γ'' coarsening. In contrast, the microstructural degradation in DT706 was retarded as compared to Inconel 706, although the formation of η phase was not completely suppressed.

Keywords: IN706, Chemistry modification, microstructure, SEM, TEM, 3DAP

1. Introduction

Although initially conceived as material for gas-turbine components in the aerospace industry, alloy 706 has been successively developed to substitute steels in large forging parts of industrial gas turbines [1, 2]. This development was driven by the quest for higher efficiencies in the electric utility sector, which requires higher operating temperatures and larger machines. Nonetheless, it has provided extreme challenges to the metal processing industry, since the size of the forgings for land based gas turbines exceeds the largest aircraft engine by almost an order of magnitude [3]. The recent need for increased efficiency in the steam turbine industry could jack up the development of 706 one step further. For instance, the objective of the European THERMIE project is to develop an ultrasupercritical (USC) steam turbine operating with steam inlet temperatures of 700°C and higher, aiming at a thermodynamic efficiency of approximately 55% (today 48%). As steam turbine components are uncooled, substitution of currently employed ferritic steels in the hottest turbine sections constitutes a complex proposition. The use of Ni-base wrought superalloys appears as a logical consequence, but indeed the transition from gas turbine to steam turbine uses is not a straightforward enterprise as it may seem. Several challenging requirements are in fact introduced, outpacing significantly the aeroengine needs. In particular, two aspects are of dominant importance: the capability of manufacturing very large forgings (up to 50 tons) and an exceptional long term stability of the microstructure in the aimed temperature range, to ensure stable mechanical performance over the entire operating life of the power plant. Among the commercial wrought nickel-iron-base superalloys, Inconel 706 stands out for this application because it combines high mechanical strength with good fabricability and

machinability. These properties directly relate to the precipitation hardening system of alloy 706, which provides the desirable characteristic of delayed the hardening response during exposure to precipitation temperatures [4]. Similarly to alloy Inconel 718, from which Inconel 706 is derived, the primary precipitation hardening elements of 706 are niobium, titanium and aluminum. The balance between Niobium and Titanium has been judiciously chosen in Inconel 706 to minimize the tendency of segregation during solidification of the ingot, thus allowing the casting of larger ingots than those of Inconel 718. The austenitic Ni-Fe-Cr matrix of Inconel 706 is mainly strengthened by the precipitation of two kinds of coherent A_3B-type compounds: the tetragonal Ni_3Nb γ'' phase (bct, DO_{22} structure) and the cubic $Ni_3[Al,Ti]$ γ' phase (fcc, $L1_2$ structure). The major source of strengthening in Inconel 706 is γ'', resulting from coherency strain and caused by a relatively large lattice misfit between the tetragonal cell of γ'' and the cubic cell of the γ matrix. Further, precipitation of intergranular Ni_3Ti η (hcp, DO_{24} structure) platelets can occur in some heat treatment conditions. The η precipitation is reported to stabilize the grain boundaries against environmental embrittlement and enhances the creep crack growth resistance of Inconel 706 up to three orders of magnitude compared to the unstabilized material [5].

Although Inconel 706 exhibits an excellent manufacturability and adequate mechanical properties, a recent research study [6] has pointed out that Inconel 706 does not fully meet the stringent requirements of the aimed application. Namely, the thermal stability of 706 is insufficient for long term service at 700°C, which leads to a dramatic loss of creep and tensile strength. This deterioration is caused by the metastable character of the strengthening γ' and γ'' precipitates, which rapidly transform upon exposure at temperatures > 700°C into semicoherent η laths.

In order to overcome this impasse, a compositional modification of 706 seems to be necessary. In this article we report on two different strategies for the optimization of the microstructural stability. On the one hand, it was attempted to create a diffusion barrier in the matrix surrounding the γ'/γ'' precipitates by adding Rhenium to the standard composition of Inconel 706. Rhenium is known to effectively retard the γ' coarsening in cast single crystal Ni-Base superalloys, as it strongly partitions to the matrix. On the other hand, the chemistry of Inconel 706 was specifically refined in order to minimize the thermodynamical tendency for the transformation of γ'/γ''. As the stability of the metastable γ' phase depends, among other factors, on the [Ti+Al]/[Nb] ratio of the alloy, a new alloy composition was designed, resulting in the alloy named DT706 presented here.

This article reports on the microstructural characterisation of Inconel 706 and its two derivative variants Re706 and DT706 in the as heat treated condition as well as after an overageing treatment. In order to achieve a precise determination of the phase compositions, three dimensional atom probe (3DAP) was used to complement the measurements from conventional scanning and transmission electron microscopes (SEM and TEM).

2. Experimental

2.1 Material & Heat Treatments

The compositions of the alloys used for this study are given in Tab. 1. The samples of Inconel 706 were cut from a triple melted (VIM, ESR and VAR) and forged turbine disc supplied by Alstom Ltd. Switzerland. DT706 samples were sectioned from a double melted (VIM+VAR) forged bar (final dimensions: 65 x 30 x 900 mm^3) manufactured by Saarschmiede GmbH, Germany. The Re-modified alloy Re706 was a ~ 0.3 kg ingot manufactured in our laboratory. The ingot was VIM melted and cast into a plate-shaped mould. In order to achieve a full recrystallization in the subsequent stabilizing and ageing heat treatment, the plate was first

homogenized under vacuum in three steps (1253 K / 1h, 1353 K/1h and 1453 K/1h), then cold rolled by a number of passes from 3 mm to 2 mm thickness.

Table 1: Chemical composition of the investigated alloys in wt. %.

	Ni	Fe	Cr	Nb	Ti	Al	Re	C
IN706	41.96	36.93	16.01	3.06	1.56	0.21	-	0.01
Re706	45.6	31.3	15.8	3.13	1.69	0.29	1.96	0.01
DT706	53.7	22.72	17.96	3.01	1.84	0.57	< 0.1	0.01

Each block of material was initially heat treated according to the so called modified stabilization treatment (MST) cycle. This heat treatment, derived from the standard stabilization heat treatment (ST) for Inconel 706 [1], was developed by Müller and Rösler [5], aiming to increase the precipitation of intercrystalline η phase. In Inconel 706, the MST treatment results in almost three orders of magnitude higher creep crack growth resistance than the ST condition. The heat treatment parameters of the MST cycle are identical for both IN706 and Re706 alloys but differ for DT706, in order to account for the effects of a slightly higher solutioning temperature due to the corresponding compositional changes. Further, the precipitation ageing step, consists only of a single ageing at 993 K for DT706 (instead of the double aging at 993 K and 893 K for IN706 and Re706). All heat treatments are listed in Table-2.

Table 2: Heat treatment parameters.

	Solutioning	Stabilization	Ageing
IN706, Re706	1253 K / 3h with 240 K / h FC to 1093 K	1093 K / 10 h FC to RT	993 K / 8 h, with 60 K / h FC to 893 K / 8h AC to RT
DT706	1353 K / 3h with 240 K / h FC to 1108 K	1108 K / 10 h FC to RT	993 K / 8 h, AC to RT

In order to simulate the microstructural changes that may occurr on long exposure at the service temperature of the prospected steam turbine components, samples of the investigated alloys were annealed at 1023 K for 5000h. This accelerated treatment aims to artificially approximate the "mid-of-life condition" of a steam turbine (that is 10,000h at 973 K) by assuming a Larson-Miller parameter $P_{LM} = T(22 + \log t)$, with the temperature T in K and the time t in h [6].

2.2 Metallography

Specimens for scanning electron microscopy were prepared by conventional mechanical grinding and polishing. The IN706 and DT706 samples were etched with the "V2A-Beize" mixture [8] at a temperature between 333 K and 343 K. For SEM imaging of the Re706 samples a mixture of 100 ml distilled water, 100 ml HNO_3 (65%), 100 ml HCl (37%) and 3 g of MoO_3 (85%) at ambient temperature was used as etchant. Foils for transmission electron microscopy were prepared by twin jet-polishing at 258 K with a solution of 30 ml ethylene-glycol monobutyl ether, 63 ml ethanol and 7 ml $HClO_4$. A Leo 1550 Gemini SEM with field emission gun and in-lens detector, and a point to point resolution of 3 nm and a Philips CM 12 TEM operating at an acceleration voltage of 120 kV was used for microstructural studies.
The Vickers hardness of the samples was measured according to EN 6507-1, applying a load of 98.1 N for 30 s.

2.3 3-Dimensional Atom Probe (3DAP)

The samples used for 3DAP analyses were cut into rods of 0.2 x 0.2 x 10 mm^3. From these rods tips with radius < 50 nm were prepared by electropolishing in two steps: first in a solution of 15 % perchloric acid in 85 % acetic acid and second in an electrolyte of 2 % perchloric acid in butoxyethanol. The 3DAP analyses were performed in vacuum of 10^{-8} Pa at a temperature of 60 K with a pulse fraction of 20 % and a pulse repetition rate of 1kHz. A CAMECA Three-Dimensional Tomographic Atom Probe was employed.

3. Results

3.1 Electron Microscopy

Microstructures after MST heat treatment

The microstructure of IN706 after the MST heat treatment is presented in fig. 1. The majority of the grain boundaries are decorated with discontinuous platelets having length between 0.5 µm and 3 µm. These particles were identified as hexagonal η phase from the analysis of the selected area diffraction pattern. The composition of the plates (measured by EDS in TEM, see Tab. 3) differs from the stoichiometric Ni_3Ti formula, revealing a large solubility for Nb and other elements such as Fe, Cr and Al. A small fraction of thin needles of η phase is also precipitated in the grain interior. The matrix is mainly hardened by a dispersion of fine γ'/γ" particles, as shown in figure 2. They are present in two morphologies, the "compact" type (consisting of a cuboidal γ' particle mantled on all six facets by shells of γ") and the "non-compact" type (i.e., a core of γ' sandwiched between two discs of γ"). The fraction of non-compact co-precipitates prevails over the compact type. Besides, larger co-precipitates consisting of a coarse γ" disc in epitaxy with an elongated γ' particle are also dispersed in the matrix (see fig. 2).

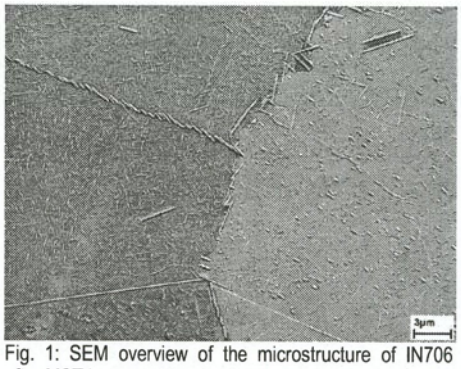

Fig. 1: SEM overview of the microstructure of IN706 after MST heat treatment.

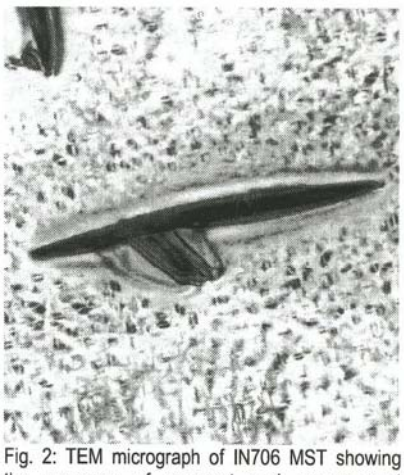
Fig. 2: TEM micrograph of IN706 MST showing the presence of compact and non-compact γ'/γ" co-precipitates. Also visible is a large γ" disc to which a γ' particle is attached.

An overview of the DT706 microstructure is given in fig. 3. The grain boundaries are decorated by cellular η precipitates, which form in some cases large nodules extending into the grain interior. A TEM image of the intragranular structure is shown in fig. 4, displaying a bimodal particle distribution. The larger particles are primary precipitates formed during the η-stabilization step at 1108 K, whereas the finer particles (secondary precipitates) have formed during the final ageing at 993 K. The γ'/γ" particles are generally larger in size and more widely spaced than in IN706. Although both the compact and the non-compact γ'/γ" types have precipitated in DT706, the major fraction of γ'/γ" co-precipitates are of the compact morphology, in

contrast to IN706. No coarse γ'/γ" precipitates were found in DT706. A detailed characterization of the precipitation behaviour of DT706 alloy is reported in [9].

Table 3: Phase composition in at. %, detected by EDS analysis.

Phase	Ni	Fe	Cr	Nb	Ti	Al	Re
η IN706	71.4 ± 1.35	5.7 ± 0.55	1.0 ± 0.55	7.5 ± 0.45	13.5 ± 0.43	-	-
η Re706	62,25 ± 1,0	10,29 ± 1,7	3,13 ± 0,9	8,9 ± 1,2	14,2 ± 1,2	1,16 ± 0,3	0,09 ± 0,07

A SEM image of Re706 is shown in fig. 5. Two types of particles are precipitated intergranularly in this alloy: discontinuous platelets and rounded / blocky particles. The compositions of these particles were analysed by EDS in the SEM. The platelets are identified as $Ni_3(Ti,Nb)$ η phase, whereas the blocky precipitates exhibit an A_2B stoichiometry that can be ascribed to the Laves phase. TEM bright field image and selected area diffraction pattern (SAD), shown in fig. 6, demonstrates that γ'/γ" precipitates are also present in this alloy. However, they are significantly finer than in IN706 and DT706, and are consequently not visible in fig. 5. Due to their extremely small size, a precise determination of the precipitate / co-precipitate morphology was not attempted.

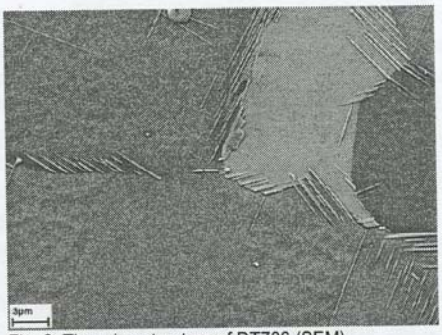

Fig. 3: The microstructure of DT706 (SEM).

Microstructures after overageing

The structure of the MST heat treated Inconel 706 after overage annealing (5000h at 1023K) is shown in Fig. 7. While the intergranular structure does not manifest an evident coarsening as compared to the initial heat treated state, the intragranular γ'/γ" particles have completely transformed into η laths, having a Widmanstätten morphology.

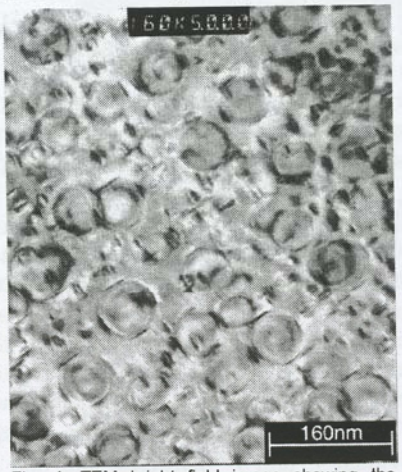

Fig. 4: TEM bright field image showing the distribution of the γ''/γ'' precipitates in DT706.

The overaged microstructures of the DT706 and Re706 samples are presented in figures 8 and 9, respectively. Although both experimental alloys show degradation of the initial microstructure, the

Fig. 5: SEM micrograph of the Re706 sample.

state of coarsening and phase transformation differ from each other. In DT706 only a relatively moderate fraction of the original γ' particles has transformed into η phase after overageing, while the remaining γ' precipitates have grown to a size of about 250 nm, as further documented in fig. 10. The shells of γ", which originally covered the cuboidal γ' particles, are almost completely dissolved. Some remaining γ" phase has the morphology of relatively large discs after overageing, usually in epitaxy with γ' particles. In contrast, the grain interiors of the overaged Re706 sample exhibits a bimodal distribution of long and short Widmanstätten plates, plus a very low fraction of coarse γ' and γ" particles.

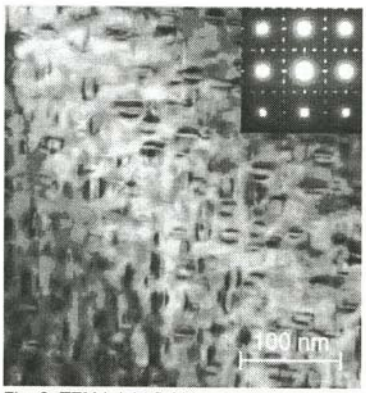

Fig. 6: TEM bright field image of Re706. The SAD pattern in the inset proves that both γ' and γ'' phases are precipitated in the matrix.

Hardness

Figure 11 shows the hardness as a function of the ageing time at 1023K for the investigated alloys. All alloys display a gradual decrease in hardness, which tends to reach a stationary value after prolonged exposure. The hardness of DT706 in the overaged condition is 74% of the initial value, compared to 62% and 57% for IN706 and Re706, respectively.

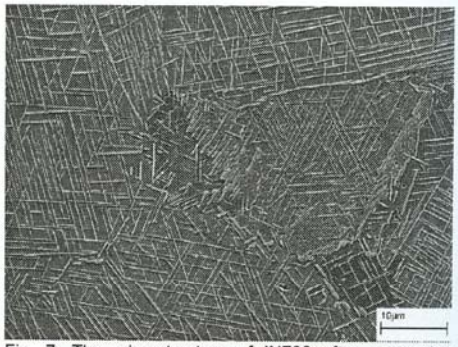
Fig. 7: The microstructure of IN706 after overageing treatment (18*10⁶ s / 1023K), taken at the SEM.

3.2 Three-dimensional Atom Probing

The composition of different γ' and γ" precipitates after MST heat treatment is measured using 3DAP. The spatial reconstruction of the atom positions detected by 3DAP allows identification of the size, the morphology and the composition of different precipitates in the investigated alloys after heat treatment, revealing sometimes the presence of fine particles which were not clearly resolved in the electron microscope. In IN706, for instance, individual γ' precipitates – but no individual γ'' - were detected by 3DAP. These particles (not seen in the TEM) are extremely small. Non-compact γ'/γ'' co-precipitates were identified, too. The examination of the precipitates in Re706 revealed a mixed distribution of individual and combined γ'/γ'' particles. The typical size of the individual γ' and γ'' particles, and that of the γ'/γ'' co-precipitates are about 10 nm. In the analysed volumes of DT706 large and

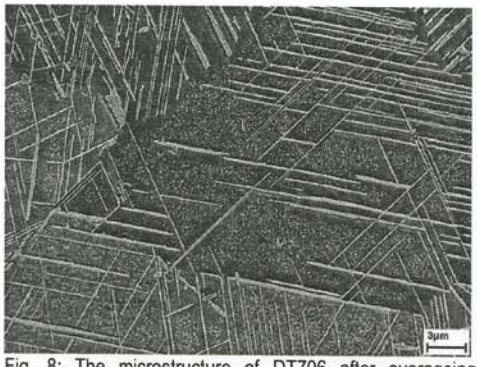
Fig. 8: The microstructure of DT706 after overageing treatment (18*10⁶ s / 1023K), taken at the SEM.

small γ′ particles, corresponding to the primary and secondary precipitates respectively, were encountered. No shells of γ" were however found in the reconstructed volumes.

Fig. 9: The microstructure of Re706 after overageing treatment (18*10⁶ s / 1023K), taken at the SEM.

The compositions of the γ' and γ" phases for the different alloys after heat treatment are listed in table 4. The γ′ phase in IN706 shows a higher concentration of Ti (~ 17 at. %), regardless of the particle morphology (individual particles or in epitaxy with γ′′). On the contrary, the Al and Nb contents of the individual and combined γ′ are slightly different. The individual γ′ particles contain 5.1 at. % Al, but the Al content is lower in the combined γ′ particle (3.5 at. %). The concentrations of Niobium in the individual and combined particles of □′ are comparable to that of Aluminium, but it shows the inverse partitioning tendency. The γ′′ composition indicates a relatively large solubility for Ti (7.0 at. %).

Table 4: Phase compositions in at. % of the investigated alloys after MST heat treatment, as measured by three-dimensional atom probe. (Ind. = individual precipitate, copr. = co-precipitate, pr. = primary precipitate, sec. = secondary precipitate).

	Ni	Al	Ti	Nb	Cr	Fe	Re
				IN706			
γ	36.8 ± 0.5	0.47 ± 0.1	1.0 ± 0.1	1.0 ± 0.1	16.1 ± 0.6	44.2 ± 0.7	
γ'_{ind}	70.1 ± 0.6	5.1 ± 0.4	17.2 ± 0.5	3.8 ± 0.3	0.4 ± 0.1	3.1 ± 0.3	
γ'_{copr}	70.2 ± 0.6	3.5 ± 0.3	17.0 ± 0.6	6.1 ± 0.3	0.7 ± 0.1	2.1 ± 0.2	
γ''_{copr}	69.9 ± 0.7	-	7.0 ± 0.3	20.6 ± 0.7	0.7 ± 0.1	1.8 ± 0.2	
				DT706			
γ	44.8 ± 0.4	0.46 ± 0.03	0.57 ± 0.01	1.8 ± 0.2	24.3 ± 0.3	28.2 ± 0.6	
γ'_{pr}	70.1 ± 0.8	8.1 ± 0.6	13.7 ± 1	4.9 ± 0.4	0.5 ± 0.1	2.7 ± 0.4	
γ'_{sec}	69.9 ± 3	8.8 ± 2	11.5 ± 2	6.2 ± 2	0.7 ± 0.4	2.8 ± 0.6	
				Re706			
	36.9 ± 1	0.36 ± 0.04	0.38 ± 0.05	0.7 ± 0.2	17.2 ± 1	43.6 ± 0.5	0.79 ± 0.05
γ'_{ind}	76.1 ± 2	3.1 ± 0.3	12.1 ± 2	5.2 ± 1	0.78 ± 0.2	2.6 ± 0.4	0.25 ± 0.1
γ'_{copr}	76.45 ± 3	3.36 ± 0.8	12.63 ± 2	4.67 ± 1	0.38 ± 0.2	2.31 ± 0.3	0.20 ± 0.1
γ''_{ind}	75.26 ± 2	0.11 ± 0.1	9.15 ± 1	12.92 ± 2	0.63 ± 0.3	1.62 ± 0.9	0.32 ± 0.2
γ''_{copr}	75.02 ± 3	0.1 ± 0.1	8.77 ± 2	13.33 ± 3	0.85 ± 0.3	1.66 ± 0.6	0.274 ± 0.2

The compositions of the γ′ and γ′′ phases in Re706 differ only marginally from IN706. The γ' precipitates (both individual and the co-precipitates) have higher Ni but lower Ti. The three-dimensional reconstruction of the various atom distribution shows that the matrix has 3-4 times higher Re content than in the γ' precipitates, and the spatial distribution of Rhenium in the matrix is not homogeneous. However, no preferential Re enrichment at the γ/γ' interfaces were observed.

The results of the 3DAP analysis of DT 706 are listed in Table 4, too. The average compositions of the primary and secondary γ' precipitates are similar, as the differences between the two kinds of particles are maintained within the statistical uncertainties. The γ′ particles contain a similar amount of Ni and Nb as in IN706, but about 5 at.% more Al and correspondingly less Ti.

The concentration ratios (γ/γ') of the various elements for different precipitate morphologies in different alloys are listed in table 5. It may be noted that these values are not partitioning ratios, since the alloys contain more than two phases.

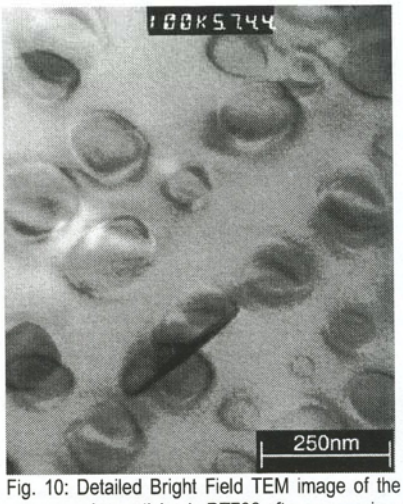

Fig. 10: Detailed Bright Field TEM image of the transgranular particles in DT706 after overageing.

Table 5: γ/γ' Concentration ratios for the different alloying elements calculated from the data presented in table 4.

	Ni	Al	Ti	Nb	Cr	Fe	Re
				IN706			
$\gamma/\gamma'_{ind.}$	0.5	0.09	0.06	0.27	40	14.3	/
$\gamma/\gamma'_{copr.}$	0.5	0.13	0.06	0.16	23	21	/
				DT706			
γ/γ'_{pr}	0.64	0.06	0.04	0.37	48.6	10.4	/
				Re706			
$\gamma/\gamma'_{ind.}$	0.48	0.12	0.03	0.13	22.1	16.8	3.16
$\gamma/\gamma'_{copr.}$	0.48	0.11	0.03	0.15	45.2	18.9	3.95

4. Discussion

The microscopic investigations on Inconel 706 demonstrated that the overageing treatment chosen for this study (which is presumed to approximately simulate the effects of a thermal exposure corresponding to the mid of life condition of a steam turbine disk), leads to an extreme deterioration of the initial microstructure. As the hardening γ' and γ" particles transform into long laths of η phase after 5000h at 1023 K, the mechanical strength of the alloy is dramatically affected. This softening effect is confirmed by the hardness measurements, which shows that the hardness in the overaged state of IN706 is only approx. 2/3 of that in the as heat treated condition.

In contrary to the expectations, the Rhenium modified variant of Inconel 706 does not show a significant increase of the thermal stability. The amount of remaining γ'/γ" precipitates after the overageing treatment is small and the final hardness of Re706 is almost the same as that of IN706. A possible explanation is offered by the results of the 3DAP investigations. It was shown that the partitioning of Rhenium between γ / γ' is not as strong as in the case of new generation single crystal superalloys [10]. In Re706 the matrix has only about 2 to 3 times more Re than in the γ' phase. Further, the Re atoms do not tend to accumulate in the region surrounding the γ/γ' interfaces in the matrix side, and thus do not effectively hinder precipitate growth. The results of this study therefore suggest that alloying with Re is not the right choice in order to stabilize the structure of Ni-Fe wrought superalloys such as Inconel 706.

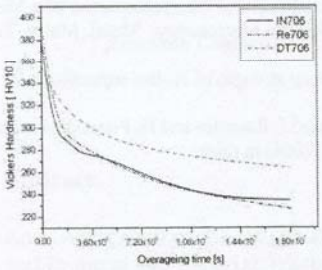

Fig. 11: Hardness profiles of the tested alloys as a function of the overageing exposure at 1023 K.

On the other hand, it was observed that the thermal stability of DT706 is significantly improved. Although the γ' particles have coarsened to larger sizes and have also partly transformed into η phase, a significant fraction of them is retained even after the overageing treatment, thereby preserving a substantial part of the initial strength of the matrix. The improvement is mainly ascribed to the change in composition of the matrix and the precipitate phases which thermodynamically stabilize the γ' phase in DT706. It also leads to a lower γ / γ' lattice misfit value compared to that in Inconel 706 [11]. Beside this aspect, other microstructural factors, like different precipitate morphology and distribution of the γ'/γ" co-precipitates, or the lower fraction of the γ" phase, could also have an influence on the improved stability of the microstructure. The encouraging results demonstrate that the design concept of DT706 represents a successful step forward in the development of new 706 chemistry to meet the requirements of the USC steam turbine application.

5. Acknowledgements

The authors are grateful to the Deutsche Forschungsgemeinschaft (DFG) for the financial support for the Projects: Wa-1378/5-3 and Rö 2045/12-3. Thanks are also due to Alstom LTD, for the kind supply of the IN706 material.

References

[1] P.W. Schilke, R.C. Schwant, Alloy 706 use, process optimization, and future directions for GE gas turbine rotor materials, Superalloys 718, 625, 706 and Various Derivatives, (2001), pp. 25-34.
[2] H.L. Eiselstein, Properties of Inconel alloy 706, ASM tech. Rep. No. C 70-9.5 , Metals Park, Ohio, (1970), pp. 1-21.
[3] S. V. Thamboo, R. C. Schwant, L. Yang, L. A. Jackman, B. J. Bond, R. L. Kennedy, Large diameter 718 ingots for land-based gas turbines, Superalloys 718, 625, 706 and Various Derivatives, (2001), pp. 57-70.
[4] Inconel alloy 706 (technical broschure), Huntington Alloys Inc., (1974).
[5] J. Rösler, S. Müller, D. Del Genovese, M. Götting, Design of Inconel 706 for Improved Creep Crack Growth Resistance, Superalloys 718, 625, 706 and Various Derivatives, (2001), pp.523-534.
[6] J. Rösler, M. Götting, D. Del Genovese, B. Böttger, R. Kopp, M. Wolske, F. Schubert, H.-J. Penkalla, T. Seliga, A. Thoma, A. Scholz, C. Berger, Wrought Ni-Base Superalloys for Steam Turbine Applications beyond 700 °C, Advanced Engineering Materials, Volume 5, (2003), pp. 469 – 483.

[7] D. Mukherji, P. Strunz, D. Del Genovese, R. Gilles, J. Rösler; A. Wiedenmann, Investigation of microstructural changes in INCONEL 706 at high temperatures by in-situ small-angle neutron scattering, Metal. Mater. Trans. A, 34A, (2003), pp. 2781-2792.
[8] G. Petzow, Metallographisches, keramographisches, plastographisches Ätzen, (1994), p. 241.
[9] D. Del Genovese, P. Strunz, D. Mukherji, R. Gilles, J. Rösler, Microstructural Characterization of a Modified 706-type Ni-Fe Superalloy by Small-Angle Neutron Scattering and Electron Microscopy, Metal. Mater. Trans. A, 36A, (2005), pp. 3439-3450.
[10] D. Mukherji and J. Rösler, Effect of the γ' volume fraction on the creep strength of Ni-bae superalloys, Z. Metallkd. **94** (2003) 478-484
[11] M. Hoelzel, D. Del Genovese, R. Gilles, D. Mukherji, D.M. Toebbens, J. Roessler and H. Fuess, Phase analysis and lattice mismatches in superalloys DT706 and Iconel 706, Physica B (2006) in print.